Dynamic Footprint-Based Person Recognition Method Using a Hidden Markov Model and a Neural Network

Jin-Woo Jung,[1,*] Tomomasa Sato,[2,†] Zeungnam Bien[1,‡]
[1]*Department of Electrical Engineering and Computer Science, Korea Advanced Institute of Science and Technology, 373-1 Guseong-dong, Yuseong-gu, Daejeon, Korea*
[2]*Department of Mechano-Informatics, University of Tokyo, 7-3-1 Hongo, Bunkyou-Ku, Tokyo, Japan*

Many diverse methods have been developed in the field of biometric identification as a greater emphasis is placed on human friendliness in the area of intelligent systems. One emerging method is the use of footprint shape. However, in previous research, there were some limitations resulting from the spatial resolution of sensors. One possible method to overcome this limitation is through the use of additional and independent information such as gait information during walking. In this study, we suggest a new person-recognition scheme based on the center of pressure (COP) trajectory in the dynamic footprint. To make an efficient and automated footprint-based person recognition method using the COP trajectory, we use a hidden Markov model and a neural network. Finally, we demonstrate the usefulness of the suggested method, obtaining an approximately 80% recognition rate using only the COP trajectory in our experiment with 11 people. © 2004 Wiley Periodicals, Inc.

1. INTRODUCTION

To date, there has been rapid growth in the field of person identification techniques for the purpose of security and personalized services. Among the various methods of person identification, biometric identification such as fingerprints or iris scans is currently the most promising method.[1–3]

These techniques can be divided into two categories: (1) high accuracy-oriented methods for the application of security in an unspecified number among

*Author to whom all correspondence should be addressed: e-mail: jinwoo@ctrsys.kaist.ac.kr.
†e-mail: tomo@ics.t.u-tokyo.ac.jp.
‡e-mail: zbien@ee.kaist.ac.kr.

INTERNATIONAL JOURNAL OF INTELLIGENT SYSTEMS, VOL. 19, 1127–1141 (2004)
 • DOI 10.1002/int.20040

the general public and (2) easy-to-use approaches for the application of personalized service in a specified number of specific small group members such as coworkers or family.[4]

Automatic face recognition,[5] gait recognition,[6,7] and footprint recognition[8,9] are representative easy-to-use methods. Specially, for applications in residential environments such as personalized services, the footprint-based person recognition method has some advantages in terms of privacy and light conditions compared with camera-based techniques such as face recognition or gait recognition.

Thus far, studies about footprints have mainly focused on medical diagnosis.[10] The possibility of footprint-based person recognition was suggested by Kennedy[11,12] and the first automatic footprint recognition scheme was developed by Nakajima et al.[8,9] using a pressure sensing mat. Kennedy[11] showed that 3000 people could be identified clearly with 38 features from inked barefoot impressions. The features that Kennedy used were mainly local features such as the distance between each toe and heel. As such, we can consider the information of toes as an important characteristic for person recognition. Nakajima et al.[8] showed a recognition rate of 82.64% among 10 people using only normalized footprint images and showed the highest rate of 86.55% additionally using the distance and angle of two feet and weight information.[9]

Figure 1 shows footprint images included in Kennedy's paper[11] and Nakajima et al.'s paper.[8] From Figure 1b, we see that the distortion by the spatial resolution of the pressure sensor is very severe, and hence toe information is difficult to extract from a footprint. Therefore, to make an automated person-recognition system with a high recognition rate, additional information is necessary. Furthermore, the size of the foot varies about 5 mm between the morning and the evening[8] and the volume also varies about 4.4%[13] between the morning and the evening. For these reasons, the use of only a footprint shape appears to have limitations.

Figure 1. Comparison of previous works: Kennedy's data[11] and Nakajima's data.[8]

In this article, we propose a different approach based on the center of pressure (COP) trajectory in a dynamic footprint. A dynamic footprint is a sequence of footprints during a single gait cycle. As such, it can be understood as gait information projected on a floor. Because the human gait is believed to be a unique individual characteristic,[2,3] we speculate that dynamic footprint-based person recognition may be possible. In Section 2, we explain the extraction process of COP trajectory from dynamic footprint images and we present a hidden Markov model (HMM) and neural network (NN)-based recognizer in Section 3. Finally, we test our recognizer using 11 people and discuss the results in terms of false rejection and false acceptance rates.

2. FEATURE EXTRACTION

On the floor, human walking can be represented by two types of information: (1) *change of contact area* and (2) *change of contact pressure distribution*. To represent this information simultaneously, we use a COP trajectory. Generally, a COP trajectory has more information than a center of area (COA) trajectory because the position of COP is determined by three-dimensional information (in contrast, the position of COA is determined by two-dimensional information).

To extract the COP trajectory for each foot during natural walking, we use a mat-type pressure sensor (MAT sensor). A MAT sensor is more acceptable than a shoe-type pressure sensor because it does not need to be worn by the subject, and it is also more robust to noise than the shoe-type sensor because it is fixed on the floor. In addition, because the pressure distribution can be represented by a gray-valued image in the MAT sensor, we can easily use the shape information of the footprint for the alignment of the COP trajectory with well-known digital image processing techniques. The drawback of a MAT sensor is that it is difficult to determine the reference point (or starting point) of the COP trajectory.

In addition, because the shape of the left foot is typically different from that of the right foot,[14] walking patterns of each foot can be asymmetric. For this reason, we use the left and right footprints together instead of a single footprint. Here, a dynamic footprint is defined as a sequence of footprints during a single gait cycle. So, it includes both the left foot and right foot simultaneously. Figure 2 shows an example of a dynamic footprint. To use each foot's information separately in the dynamic footprint, we need a discrimination procedure of the left foot and the right foot, and a procedure for making a COP trajectory of each foot.

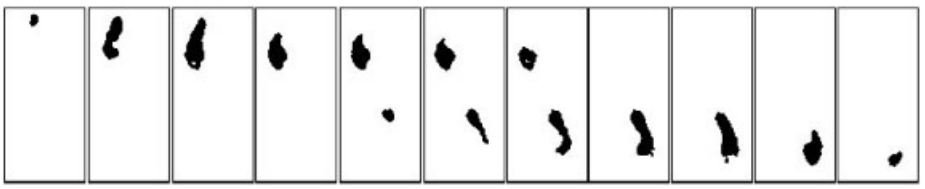

Figure 2. Example of a dynamic footprint.

2.1. Extraction Procedure of the COP Trajectory of Each Foot in the Dynamic Footprint

In this section, we describe a procedure to obtain the aligned COP trajectories of each foot in the dynamic footprint in the aspect of position and direction. The alignment process of COP trajectories of each foot is essential in the case of the MAT-type pressure sensor because the reference point (or starting point) of the COP trajectory is not fixed and the walking direction of each foot is different within the walking direction of humans, even if they already know how to walk.

For the alignment process, we use assumptions as follows:

(A-I) There is no other object on the MAT sensor except the walking person.
(A-II) There is only one walking person on the MAT sensor in each trial.
(A-III) During one's walking on the MAT sensor, at least one element of the MAT sensor is fired.
(A-IV) Normally, the user always walks along the designated direction (e.g., outdoor to indoor) on the MAT sensor.
(A-V) The user's step length (the distance between the COA point of the first foot and that of the second foot) is greater than a predefined maximum foot length, L_{MAX_FOOT}.
(A-VI) The "two" footprints are always acquired after a single gait cycle.
(A-VII) The user has to walk on the MAT sensor without wearing any shoes (i.e., barefoot walking is assumed).
(A-VIII) People who may sometimes drag their foot one after another are excluded from the subjects.

By assumptions (A-I) and (A-II), we can find the starting time of the dynamic footprint, $t_{FIRST\_FOOT\_START}$, by checking when the total pressure value is greater than the threshold value. Assumption (A-III) indicates that the total pressure value is always greater than the threshold value during a single gait cycle. This assumption (A-III) is a constraint of maximum walking speed and is generally valid during walking, but not during running. And, by assumption (A-III), we can check the ending time of the dynamic footprint, $t_{SECOND\_FOOT\_END}$. After all, by assumptions (A-I), (A-II), and (A-III), we can find $t_{FIRST\_FOOT\_START}$ and $t_{SECOND\_FOOT\_END}$ of the dynamic footprint.

Assumption (A-IV) helps us easily to find the reference direction for directional alignment of each foot. If assumption (A-IV) is not used, we should find the reference direction by another way such as averaging the walking directions of two feet. But, in some cases in which walking patterns for each foot are severely asymmetric, it is not easy to determine the human walking direction.

Assumption (A-V) is for discriminating the left foot and the right foot part in the dynamic footprint. Here, maximum foot length, L_{MAX_FOOT}, is determined according to the analysis of the user group. In our experiment, L_{MAX_FOOT} is determined as 300 mm. Assumption (A-VI) is to except the special case that one of the footprints is not perfectly included in the MAT sensor.

Finally, assumptions (A-VII) and (A-VIII) constrain the range of the subjects and the condition of the experiment.

The procedure for extracting the COP trajectory of each foot in the dynamic footprint is as follows:

At time t, $t_{FIRST\_FOOT\_START} \leq t \leq t_{SECOND\_FOOT\_END}$: Execute from Step 1 to Step 6

Step 1: Labeling of each blob. We make a label for each blob in the current footprint image using the scanning line method.[8] When the scanning line meets a segment, a number is given to the segment.

Step 2: Finding COA point of each blob. We find COA points of all labeled blobs. The COA points are used to determine whether the current blob is a part of the first foot or the second foot. We used COA point instead of COP point to make a representative point for each blob because a foot shape plays a key role in discriminating the first foot and the second foot rather than a pressure distribution.

Step 3: Discrimination of the first foot and the second foot. A k-means clustering algorithm is used to discriminate the first foot and the second foot. At $t_{FIRST\_FOOT\_START}$, we assume that the COA point of the current blob as a part of the first foot. Then if the distance between the current blob's COA point and the previous COA point of the first foot is greater than the maximum foot length L_{MAX_FOOT}, the current blob is considered as a part of the second foot. After this, we can determine whether the current blob is a part of the first foot or that of the second foot by measuring the distances between the COA point of the current blob and the allocated COA points of the first foot and the second foot. Finally, we reestimate the first foot's COA point and the second foot's COA point with these additional blobs.

Step 4: Checking whether the time of current frame, t, is $t_{FIRST\_FOOT\_END}$ or $t_{SECOND\_FOOT\_START}$. We determine $t_{FIRST\_FOOT\_END}$ by using the number of blobs in the first foot ($t_{SECOND\_FOOT\_START}$ is determined from the second foot). If there is no blob of the first foot at time t_F and there was more than one blob at time $t_F - 1/F$, then $t_{FIRST\_FOOT\_END} = t_F - 1/F$. Here, F stands for the frame rate of the MAT sensor. Similarly, if there is more than one blob of the second foot at time t_S and there was no blob of the second foot at time $t_S - 1/F$, then $t_{SECOND\_FOOT\_START} = t_S$. This process is valid under assumption (A-III).

Step 5: Updating the COP trajectory of each foot. We calculate the COP points of the first foot and the second foot. These COP points are used to update the COP trajectory of the first foot and the COP trajectory of the second foot.

Step 6: Updating an overlapped footprint image. We update the overlapped footprint image by doing OR operations on all partial footprint images during $t_{FIRST\_FOOT\_START} \leq t \leq t_{SECOND\_FOOT\_END}$. After OR operations, each overlapped footprint image is converted to a binary-valued image.

At time $t = t_{SECOND\_FOOT\_END}$: Execute from Step 7 to Step 8.

Step 7: Determination of the orientation of each foot using the principal axes of the overlapped footprint image. We find the principal axes of each foot using the overlapped footprint images of each foot. The principal axes of a region are the eigenvectors of the covariance matrix obtained by using the pixels within the region as random variables.[15] To find the principal axes of the left foot $L(x, y)$, we translate all footprint data of the left foot to $L(x', y')$ so that its COA is located in the origin. We make a covariance matrix H_L using $L(x', y')$ as in Equation 1. Then, eigenvectors e_{L1} and e_{L2} of H_L, whose eigenvalues were ordered highest to lowest, are the major and minor axes, respectively.

$$H_L = \begin{pmatrix} \sum_{x',y'} L(x',y')x'^2 & \sum_{x',y'} L(x',y')x'y' \\ \sum_{x',y'} L(x',y')x'y' & \sum_{x',y'} L(x',y')y'^2 \end{pmatrix} \tag{1}$$

Step 8: Creation of the aligned COP trajectory. We translate the original COP trajectory so that the starting point of the trajectory becomes the origin and we rotate the translated COP trajectory to $<e_{L2}$ (or $<e_{R2}$) degrees for directional alignment. The directionally aligned COP trajectory is represented as follows:

$$TRAJ_{FIRST\_FOOT}(t) = [x\ y]^T, \quad \text{where } t_{FIRST\_FOOT\_START} \le t \le t_{FIRST\_FOOT\_END}$$

$$TRAJ_{SECOND\_FOOT}(t) = [x\ y]^T, \quad \text{where } t_{SECOND\_FOOT\_START} \le t \le t_{SECOND\_FOOT\_END}$$

2.2. Characteristics of the COP Trajectory

From 11 subjects, we obtained COP trajectories of two feet during natural walking. The average weight and height of all subjects are 67.0 (±15.2) kg and 170.4 (±6.4) cm. As a MAT sensor, we used FOOT ANALYZER (TechStorm Inc., Korea) as shown in Figure 3. The size of the sensor is 80×40 cm^2 including 80×40 sensors (1×1 cm^2 resolution) and the frame rate is 30 Hz. In each trial, each subject gives 10 dynamic footprints using the MAT sensor. During 2 months, 40 dynamic footprints are acquired from each subject.

Figure 4 shows the aligned COP trajectories of subjects whose foot size is between 245 mm and 265 mm. Figure 5 is the aligned COP trajectories of a subject during 2 months. In Figures 4 and 5, the upper two figures represent two-dimensional projections of the COP trajectories for the left foot and the right foot, and the two lower figures represent three-dimensional COP trajectories with time information in the dynamic footprint. In every case, the origin is the first COP point of each foot in the COP trajectories.

Figure 3. A mat-type pressure sensor, FOOT ANALYZER.

From the real COP trajectories, we can observe interesting characteristics of COP trajectories of each foot as follows:

(C-1) COP trajectory is a temporal sequence with variable length and noisy information.
(C-2) Even in the same person, the left foot and the right foot are not symmetric and have different COP trajectories for each trial.
(C-3) Even in the same person, there is severe inconsistency in the starting and ending phases of the COP trajectories. However, there is clearly a unique trend in the middle phase of the COP trajectory.
(C-4) COP trajectories show different curvatures according to the user.

The noisy information in (C-1) is mainly caused by quantization errors and inconsistent human behavior in the dynamic footprint. Based on the above four characteristics, we design a recognizer for the dynamic footprint in the next section.

3. PERSON RECOGNITION BY HMM AND NN

Because COP trajectory is a temporal sequence with variable length and noisy information (C-1), the hidden Markov model (HMM) can be a good tool as a recognizer.[16] Instead of HMM, we can also consider other dynamic programming techniques such as dynamic time warping (DTW). But, in that case, noisy information of the COP trajectory will disturb the recognition so that additional processing for noise reduction is necessary. On the other side, HMM is more robust to noise by its learning ability.

To use HMM efficiently, we need to quantize the COP trajectory. The quantization process of the COP trajectory is basically to reduce the feature dimension from two dimensions to one dimension to obtain better results with small training data. The method that we used is a kind of modified direction-based quantization method as follows:

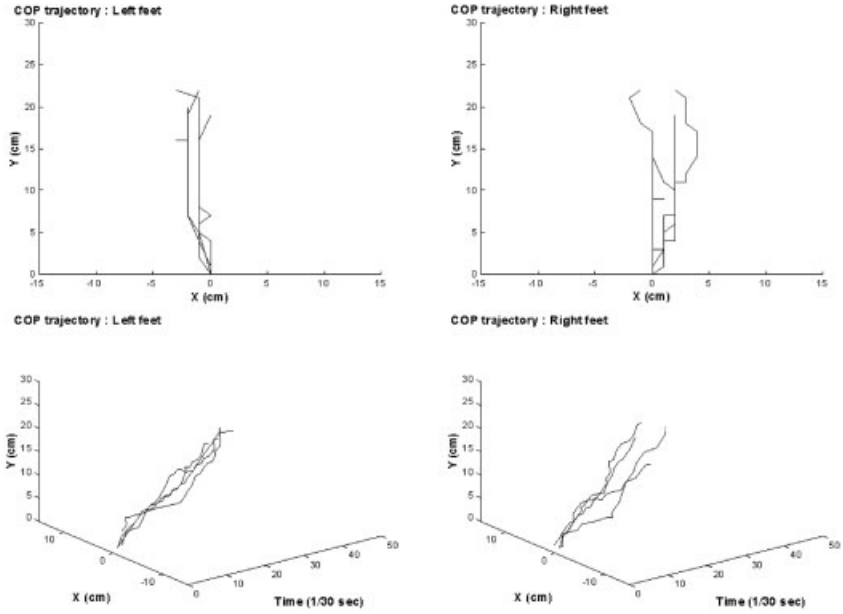

Figure 4. COP trajectories of subjects whose foot size is between 245 mm and 265 mm among 11 users.

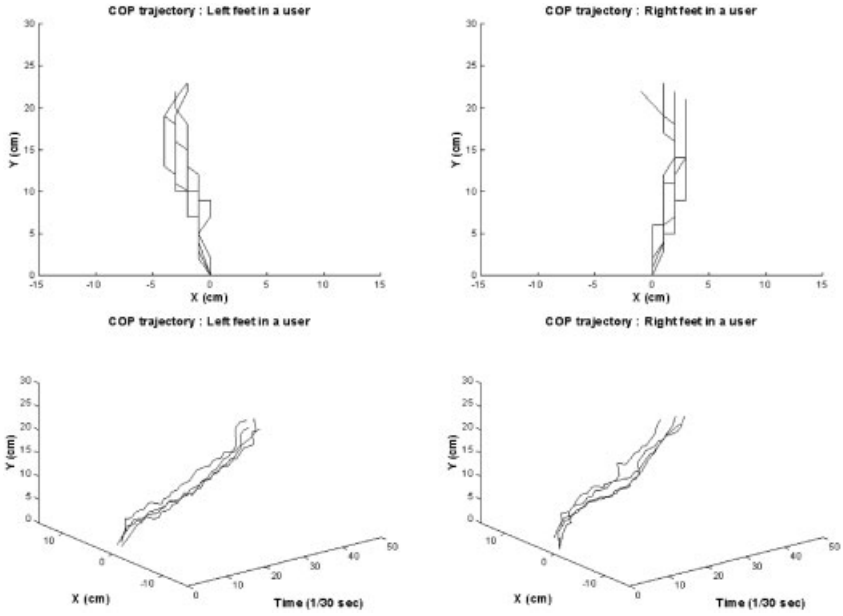

Figure 5. COP trajectories of a user during 2 months.

$$\text{Directional index } I = (f(\Delta x), f(\Delta y)) \quad \text{where } f(k) = \begin{cases} -2 & \text{if } k < -T \\ -1 & \text{if } -T \le k < 0 \\ 0 & \text{if } k = 0 \\ 1 & \text{if } 0 < k \le T \\ 2 & \text{if } k > T \end{cases} \tag{2}$$

$$\text{Quantization value } Q = \{f(\Delta x) + 2\} \times 5 + \{f(\Delta y) + 2\} + 1 \in \{1,2,\ldots,25\} \tag{3}$$

In Equation 2, directional index I indicates the difference vector of the current COP point and the previous one. Δx and Δy are the displacements in the x-axis and the y-axis, respectively. T is the threshold value of distance to discriminate a small change and a large one. And, the quantization value in Equation 3 is the output of the quantization process and will be used in the input of HMM.

Discriminating a small change and a large one using T can be an important factor in some cases when completely different curvatures are regarded as similar by HMM. For example, if we use the typical direction-based quantization method and scan the lines (A) and (B) in Figure 6 from the bottom to the top, two lines (A) and (B) can be divided as a series of directional components F(forward direction), L(left direction), and R(right direction) such as $(F, F, F, F, F, L, L, F, R, R, R, R, R, F, F, F, F)$ and $(F, F, F, L, L, L, L, L, F, F, F, F, F, F, R, F)$, respectively. And these two curvatures can be considered as the same (F, L, F, R, F) class in the learning process of HMM. For this reason, we included the distance concept like Equation 2 in the typical direction-based quantization method. T is designed by the frame rate of the MAT sensor and the walking speed of the subjects. The appropriate value of T that we found for our experimental environment is 10 mm at 30 Hz frame rate.

Because the quantized COP trajectory is sequential one-way data, we designed a left-to-right-type HMM for the recognition of each foot, as represented in

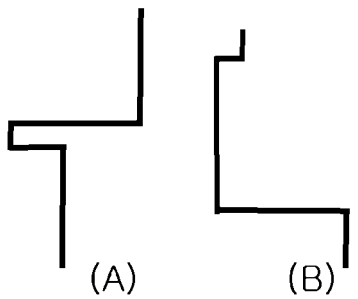

Figure 6. Two different curvatures with similar directional components.

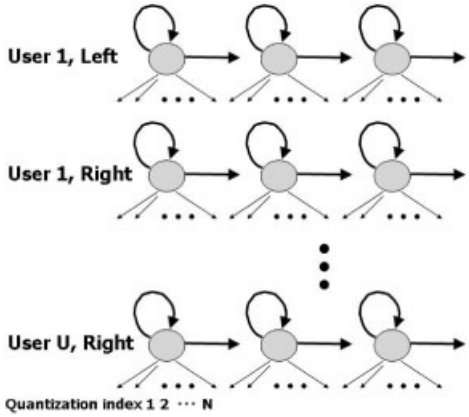

Figure 7. Hidden Markov model recognizer for each footprint.

Figure 7. In Figure 7, the node represented as a circle is a hidden state of HMM. Bold arrows indicate all possible transitions. And thin arrows are the outputs of each hidden state. Because every hidden state can make any output value among quantization values, the numbers of thin arrows in each hidden state are all the same.

Moreover, because the left foot and right foot are not symmetric and have different COP trajectories, we used two models for each person, a left foot model and a right foot model. If there are U users that we recognize, then a total of $2U$ models are used. The input of HMM is the output of the quantization procedure. The output of HMM is the probability with which the current sequence is fit to each class.

From many experiments, we observed that some people have distinctive characteristics on their left foot and other people have it on their right foot. Starting from this observation, we make a hypothesis that recognizing with a dynamic footprint using both left foot and right foot will show better performance than recognizing with single footprint data using one left or right foot. To make a dynamic footprint recognizer based on HMM, we designed a neural network (NN)-based scheme on the final decision stage for data fusion of recognition results of each footprint.

NN for final data fusion uses all HMM output data as inputs and learns the pattern of HMM output probabilities, as in Figure 8. For example, if U users are to be recognized, $4U$ HMM probability outputs are used as inputs of NN. $2U$ inputs of NN are from the results of the first foot in the dynamic footprint and other $2U$ inputs are from the second foot. And U degrees of users are the output of NN. The final decision is made by comparing the outputs of the neural network. For example, when two same degrees appear in the outputs of NN, the final decision is two users with the same degree. In this HMM-NN scheme, two kinds for learning processes are needed, learning for HMM and learning for NN.

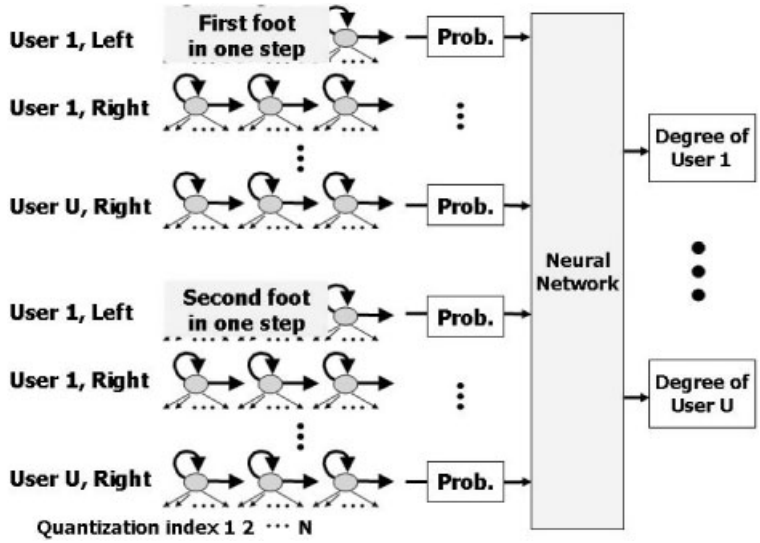

Figure 8. HMM-NN recognizer for the dynamic footprint.

Hence when the training data set is prepared, HMMs are learned first with adequate error margins. After HMM learning, the probability outputs of HMMs with the same training data become the training input of NN. Using these probabilities data, NN is learned next. For the learning of HMM, we used the well-known Baum–Welch algorithm[16] and for NN, we used the LM (Levenberg–Marquart) method.[17] The LM method is a combination of the Newton method and the standard gradient descent algorithm. The weights-updating rule is similar to Equation 4 and the step size λ was determined by an adaptive method:

$$W_{new} = W_{old} - (Z^T Z + \lambda I)^{-1} Z^T \varepsilon(W_{old}), \quad (Z)_{ni} \equiv \frac{\partial \varepsilon^n}{\partial w_i} \tag{4}$$

where ε^n is the error for the nth pattern, ε is a vector with elements ε^n, and λ is step size for learning.

4. EXPERIMENTAL RESULTS

For the performance test, we used false rejection rate (FRR) and false acceptance rate (FAR),[2,3] which are the most well-known performance measures in the biometrics area. FRR is concerned with the number of instances an authorized individual is falsely rejected by the system, as in Equation 5, and FAR refers to the number of instances a nonauthorized individual is falsely accepted by the system, as in Equation 6. Both rates are expressed as a percentage using the following calculations:

$$FRR = \frac{NFR}{NAA} \times 100\ (\%) \tag{5}$$

$$FAR = \frac{NFA}{NIA} \times 100\ (\%) \tag{6}$$

where *NFR* and *NFA* are the numbers of false rejections and false acceptances, respectively. *NAA* and *NIA* are the numbers of authorized attempts and impostor attempts, respectively.

For example, when a person (ID = M) is tested with his own COP trajectory and the final decision is falsely to be another person (ID = N), the FRR of the original person (ID = M) is increased and the FAR of the output person (ID = N) is also increased.

Equal error rate (EER) is another well-known performance measure and indicates the error when FRR and FAR have the same error value as threshold changes. So, two different recognizers generally have two different threshold degrees for EER. In this article, we used FRR and FAR instead of EER to compare various structures of recognizer in the same threshold degree, 0.5.

Table I shows various recognition errors of the HMM-NN (no hidden layer in NN) recognizer with different HMM structures and different features for the 11 subjects' data. Among 40 data during 2 months, 20 data in the first month were used as training samples and 20 data in the other month were used as test samples.

From Table I, we can find that COP trajectory is better than COA trajectory as a feature of person recognition. This can be understood as COP is more suitable to express the habitual behavior and distinguishable gait information, during each user's natural walking. As such, COA appears to be more robust than COP. The best results were found when we use the five states HMM and COP trajectory-based feature that shows 20.45% FRR and 2.05% FAR on average. This means this system achieves an approximately 80% recognition rate when we use the five states HMM and COP trajectory-based feature.

Table I. Recognition errors with different HMM structures and different features.

	COA trajectory-based		COP trajectory-based	
No. of states in HMM	Average of FRR (%)	Average of FAR (%)	Average of FRR (%)	Average of FAR (%)
3 states	38.64	3.86	28.64	2.86
4 states	33.18	3.32	27.73	2.77
5 states	33.18	3.32	20.45	2.05
6 states	37.73	3.77	31.36	3.14
7 states	32.27	3.23	30.91	3.09
8 states	33.64	3.36	31.82	3.18
Total	34.77	3.48	28.49	2.85

Table II. Recognition errors with different NN structures.

Structure of hidden layer in NN	Average of FRR (%)	Average of FAR (%)
0	20.45	2.05
3	73.18	7.32
5	55.00	5.50
7	61.36	6.14
9	54.09	5.41
11	40.45	4.05
3×3	73.64	7.36
5×5	66.82	6.68
7×7	60.45	6.05

Table II shows the recognition results with various NN structures for COP trajectory-based five states HMMs. Training and test samples were the same as presented in Table I. In this table, we can find that an NN without a hidden layer gives the best results in many HMM-NN structures. This can be explained by the following two reasons. One possible reason is that the decision boundary is not too complex because the inputs of NN are the outputs of the HMM-based recognizer. Thus the complex structure of NN yields unexpected results by over-fitting. Another possible reason is that the learning sample is not sufficiently large to learn with the complex structure of NN. However, in a real application, increasing the learning samples creates a greater burden for users. Thus, we conclude that the HMM (five states)–NN (no hidden layer) structure with the COP trajectory-based feature is the most efficient structure.

The final result, 80% recognition rate, is not sufficiently good for real applications in person recognition. However we can find another interesting result from Figures 9 and 10. Figures 9 and 10 show the decreasing effect in recognition errors,

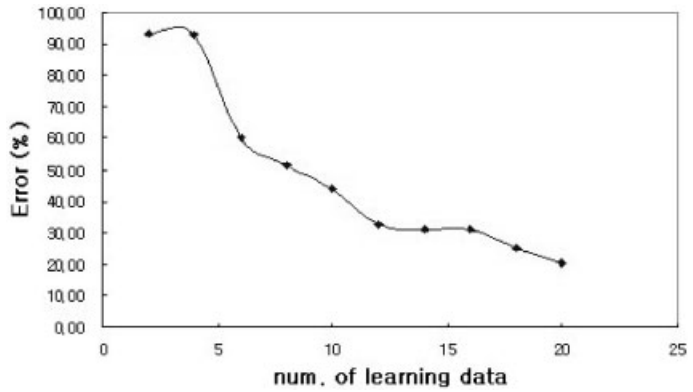

Figure 9. FRR with increasing number of learning data as time goes on.

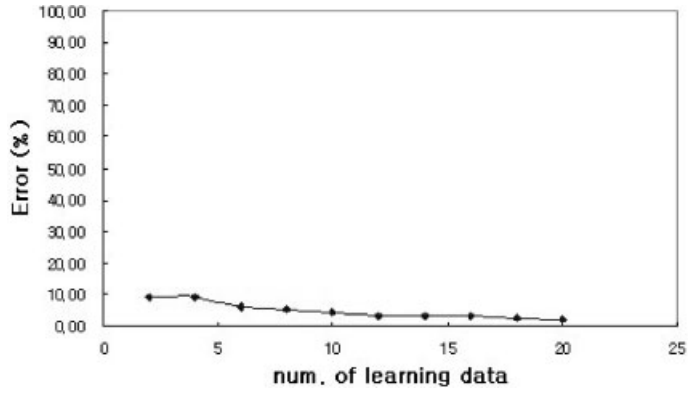

Figure 10. FAR with increasing number of learning data as time goes on.

FRR and FAR, with an increasing number of learning data as time goes on. By learning the first day's data (totally 10 learning data), FRR reduced to 43.64%, and by additionally learning the second day's data (totally 20 learning data), FRR reduced to 20.45%. Hence, if we made an on-line learning scheme, we could obtain better results over time.

5. CONCLUSIONS AND FUTURE WORK

Thus far, previous studies on footprints have focused on medical diagnosis. From Kennedy's work[11] and Nakajima et al.'s work,[8] methods for person recognition using footprint shape were developed. But, footprint shape is not good to achieve enough information by spatial resolution of sensor and variation of parameter values in the foot. So, additional information that is independent of footprint shape is necessary to make a real application with high performance.

In this article, we proposed a new person recognition method based on COP trajectory in the dynamic footprint. We suggested the extraction procedure of the aligned COP trajectory for MAT sensor and a quantization method for HMM. From the observation that the left foot and right foot are not symmetric in terms of COP trajectory, we made separate models for each foot using HMM as basic recognizers. To combine the output probabilities of HMMs during the single gait cycle, we designed the final decision method based on NN. And, we tested various structures of the HMM-NN recognizer with COP and COA trajectories.

From the obtained results, we concluded that the COP trajectory yields a better result than the COA trajectory for person recognition. In our experimental analysis with 11 subjects, the best structure was a combination type of HMM with five states and an NN with no hidden layer. And the best result was 20.45% in FRR error and 2.45% in FAR error. The recognition rate of about 80% is not sufficient for real applications, but by a fusion of previous research on footprint shape, we can expect an improvement in the recognition rate.

Acknowledgments

This work is partially supported by Human-friendly Welfare Robot System Engineering Research Center, KAIST, and the Brain-Korea 21 program of the Ministry of Education of Korea. The authors wish to thank all those individuals who volunteered their footprints for this study.

References

1. Liu S, Silverman M. A practical guide to biometric security technology. IEEE IT Pro 2001;Jan/Feb:27–32.
2. Jain A, Bolle R, Pankanti S. Biometrics—Personal identification in networked society. Dordrecht: Kluwer Academic Publishers; 1998.
3. Zhang DD. Automated biometrics—Technologies and systems. Dordrecht: Kluwer Academic Publishers; 2000.
4. Jung JW, Sato T, Bien Z. Unconstrained person recognition method using dynamic footprint. In: Proc Int Conf on Fuzzy Information Processing. Beijing: Tsinghua University Press; 2003. pp 531–536.
5. Sukthankar R, Stockton R. Argus: The digital doorman. IEEE Intell Syst 2001;16:14–19.
6. Yam CY, Nixon MS, Carter JN. Performance analysis on new biometric gait motion model. In: Proc 5th IEEE Southwest Symposium on Image Analysis and Interpretation. Santa Fe, NM: IEEE Press; 2002. pp 31–34.
7. Kale A, Cuntoor N, Yegnanarayana B, Rajagopalan AN, Chellappa R. Gait analysis for human identification. Proc AVBPA; 2003. pp 706–714.
8. Nakajima K, Mizukami Y, Tanaka K, Tamura T. Footprint-based personal recognition. IEEE Trans Biomed Eng 2000;47:1534–1537.
9. Nakajima K, Mizukami Y, Tanaka K, Tamura T. A new biometrics using footprint. Trans Inst Electr Eng Jpn D 2001;121:770–776.
10. Razeghi M, Batt ME. Foot type classification: A critical review of current methods. Gait and Posture 2002;15:282–291.
11. Kennedy RB. Uniqueness of bare feet and its use as a possible means of identification. Forensic Sci Int 1996;82:81–87.
12. Kennedy RB, Pressman IS, Chen S, Petersen PH, Pressman AE. Statistical analysis of barefoot impressions. J Forensic Sci 2003;48:55–63.
13. Nah G. Circadian changes of human stature and foot volume for young adult men. M.S. Thesis, Korea Advanced Institute of Science and Technology, 1985.
14. Sforza C, Michielon G, Fragnito N, Ferrario VF. Foot asymmetry in healthy adults: Elliptic Fourier analysis of standardized footprints. J Orthoped Res 1998;16:758–765.
15. Gonzalez RC, Woods RE. Digital image processing. London: Addison-Wesley; 1993.
16. Rabiner LR. A tutorial on hidden Markov models and selected applications in speech recognition. Proc IEEE 1989;77:257–285.
17. Bishop CM. Neural networks for pattern recognition. New York: Oxford University Press; 1995.